



Published in final edited form as:

J Mater Chem B Mater Biol Med. 2017 January 28; 5(4): 639–654. doi:10.1039/C6TB02008A.

Targeting Fibronectin for Cancer Imaging and Therapy

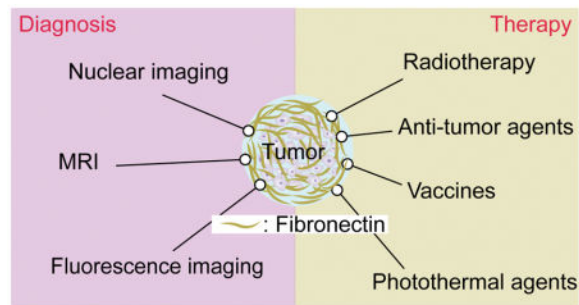
Zheng Han and Zheng-Rong Lu*

Department of Biomedical Engineering, Case Western Reserve University, 10900 Euclid Avenue, Cleveland, OH 44106, USA

Abstract

During cancer progression, the extracellular matrix (ECM) undergoes dramatic changes, which promote cancer cell migration and invasion. In the remodeled tumor ECM, fibronectin (FN) level is upregulated to assist tumor growth, progression, and invasion. FN serves as a central organizer of ECM molecules and mediates the crosstalk between the tumor microenvironment and cancer cells. Its upregulation is correlated with angiogenesis, cancer progression, metastasis, and drug resistance. A number of FN-targeting ligands have been developed for cancer imaging and therapy. Thus far, FN-targeting imaging agents have been tested for nuclear imaging, MRI, and fluorescence imaging, for tumor detection and localization. FN-targeting therapeutics, including nuclear medicine, chemotherapy drugs, cytokines, and photothermal moieties, were also developed in cancer therapy. Because of the prevalence of FN overexpression in cancer, FN targeting imaging agents and therapeutics have the promise of broad applications in the diagnosis, treatment, and image-guided interventions of many types of cancers. This review will summarize current understanding on the role of FN in cancer, discuss the design and development of FN-targeting agents, and highlight the applications of these FN-targeting agents in cancer imaging and therapy.

Graphical Abstract



Introduction

Cancer is a genetic disease and stems from gene mutation within normal cells. Based on this notion, the strategies in designing cancer imaging agents and therapeutics generally have been focused on targeting the cancer related molecular signatures existing either

*To whom correspondence should be addressed: Dr. Zheng-Rong Lu, M. Frank Rudy and Margaret Domiter Rudy Professor, Wickenden 427, Mail Stop 7207, 10900 Euclid Avenue, Cleveland, OH 44106, Phone: 216-368-0187, Fax: 216-368-4969, zxl125@case.edu.

intracellularly or on cell surface. However, it has been increasingly recognized that tumor microenvironment is a key determinant for cancer survival and progression. The extracellular matrix (ECM) of cancer is highly remodeled with a dramatic change in biochemical and physical properties. This change is accompanied by tumor-permissive immunological surroundings and recruitment of a plethora of stromal cells, including cancer-associated fibroblasts (CAFs), endothelial cells, macrophages, etc.¹ Cancer cells in the aggressive primary site are adept at exploiting the remodeled tumor microenvironment for outgrowth and invasion². Among the tumor microenvironmental cues investigated, FN stands as one of the lead cancer-related extracellular biomolecules. As an abundant molecule in ECM, FN takes part in a variety of processes that promote cancer cell progression, by interacting with cells and other ECM molecules. Over the past two decades, the role of FN in cancer has been recognized and FN-targeting strategies have been devised as promising cancer imaging and therapy approaches^{3,4}. In this article, we provide an overview of the interaction of FN with cancer cells and other ECM molecules, how this interaction correlates to cancer malignancy, and FN-targeting strategies in cancer imaging and therapy, highlighting their application in different types of cancers.

1. Upregulated fibronectin is a cancer marker

1.1 Fibronectin as an extracellular matrix molecule in tumor microenvironment

FN is an abundant, high-molecular-weight, adhesive glycoprotein that exists in the ECM or body fluids⁵. FN takes the form of dimers, joined by a pair of disulfide bonds in the carboxylic termini, the structure of which is illustrated in Figure 1. Each monomer of FN consists of three types of homologous repeats termed as type I, II and III domains. Although FN is encoded by a single gene, alternative splicing of pre-mRNA and posttranslational modifications result in the formation of cell- and tissue-specific FN isoforms. Splicing occurs at three sites, including the site located between III₁₁ and III₁₂ with the insertion of extradomain A (EDA), the site located between III₇ and III₈ with the insertion of extradomain B (EDB), and various portions of the III_{CS} domain between III₁₄ and III₁₅ (Figure 1). Splicing events result in two main FN types, soluble and insoluble FNs. Soluble FN, also called plasma fibronectin (pFN), is produced by hepatocytes and distributes in plasma (~300 µg/mL) and other body fluids⁵. Extradomains are usually absent in soluble fibronectin. Insoluble FNs, on the other hand, are synthesized by a variety of cell types, including fibroblasts, muscle cells, endothelial cells, and cancer cells. It is the product of fibrillogenesis, i.e. polymerization of FNs, which provides a multi-dimensional platform that interacts with other ECM molecules and cell surface receptors⁶.

Two FN isoforms generated by splicing in type III repeats are termed as extradomain-A fibronectin (EDA-FN) and extradomain-B fibronectin (EDB-FN). EDA- and EDB-FN are the most investigated FN isoforms for tumor-targeting strategies. EDA- and EDB-FN are expressed during embryogenesis, but their expressions are highly conservative in adult tissue except in wound healing and cancer, because of which they are called “oncofetal” fibronectins⁷. Single EDA- or EDB-FN null mice show fairly normal development but mice lacking both FN isoforms show vascular defects that results in embryonic lethality⁸⁻¹⁰.

FN plays an important role as a coordinator between ECM and cancer cells in tumor, and its upregulation facilitates cancer cell survival, proliferation, and invasion¹¹. FN is a well-established hallmark of epithelial-to-mesenchymal transition (EMT). EMT transforms cancer cells with more stem-cell-like phenotype¹², which frequently occur in the invasive front of aggressive tumors¹³ (Figure 2A). Cancer cells that undergo EMT upregulate FN along with other ECM molecules that constitute the remodeled ECM. Interestingly, secreted FN further stimulate EMT, for example, by sensitizing cancers to TGF β induction, and trigger a variety of signaling pathways that in turn upregulate FN expression^{14, 15} (Figure 2B). This feedback loop once again reflects a close alliance of FN and cancer cells. As previously mentioned, insoluble FNs are formed as a result of fibrillogenesis, which is mediated by integrin clustering¹¹ (Figure 2B). It is well known that the RGD sequence on fibronectin III₁₀ is responsible for binding cell-surface integrins¹⁶. However, RGD motif alone showed a much lower affinity to its targets than larger protein fragments of FN or intact protein. The vicinity structure of RGD, e.g. PHSRN sequence in III₉ domain, also contributes to the binding^{16, 17}. Considering that insoluble FNs distinguish themselves from soluble FN by extrodomains, it is natural to reason that these extrodomains play indispensable role in fibrillogenesis and the enhanced interaction between FN and cancer cells. It is suggested that the extradomain insertion in type III repeats results in a conformational change within FN that stabilizes head to tail dimerization of separate FN chains, which further links to FN matrix assembly¹⁸. Although the extradomain insertion does not alter integrin-binding sites, the change in conformation exposes a pair of these sites on the same face of the macromolecules, facilitating its interaction with multiple receptors on the cell surface^{17, 19}. This also enhances clustering of integrins, coupled to fibrillogenesis and a series of intracellular signaling events^{11, 19} (Figure 2B). Evidences indicate that the insertion of EDA domain may increase RGD exposure to integrins, resulting in enhanced interaction with cancer cells^{20, 21}. Meanwhile, EDA domain itself also binds to $\alpha_9\beta_1$ or $\alpha_4\beta_1$ integrins²². In terms of EDB-FN, although the receptor of EDB domain on cancer cell remains elusive, it is known that adhesion of EDB domain to cancer cell induces tyrosine phosphorylation of focal adhesion proteins, followed by activation of FAK tyrosine phosphorylation pathways²³.

FN also serves as a scaffold that provides binding sites for a variety of ECM molecules, thus making it a central organizer of ECM (Figure 2B). One of the ECM molecules directly coupled to FN is fibrin. Fibronectin, specifically plasma fibronectin (pFN), is covalently linked to fibrin²⁴. Crosslinking of FN with fibrin is a key event in clot formation. In the setting of cancer, even though pFN is reported to have no clinical correlation with cancer^{25, 26}, the presence of fibrin-fibronectin complexes (FibFN) is a characteristic of malignant cancers²⁷. A study showed that pFN-deficiency was associated with decreased metastasis in the lung, indicating a pro-metastatic effect of blood clotting *in vivo*²⁸. Further, thrombin antagonist hirudin would impair lung metastasis through inhibition of platelet activation and fibrin formation. It is suggested that this impact of FibFN complex on metastases is mediated through fibronectin- $\alpha_v\beta_3$ integrin interaction, which is absent with sole existence of pFN. However, FibFN had no effect on tumor cell growth and initial tumor cell arrest, suggesting its primary role in clotted plasma to assist in cell extravasation²⁸.

Other ECM molecules actively involved in ECM remodeling include collagen and matrix metalloproteinases (MMPs). Collagen is the most abundant protein in mammals, and is prominently overexpressed in cancer^{29, 30}. Recent studies reported the inductive function of FN in collagen deposition and architecture regulation³⁰⁻³². Accordingly, inhibition of FN matrix assembly would lead to abnormal collagen expression⁶. MMPs are essential for peritumor tissue degradation and cancer cell migration. Studies indicated a role of EDA-FN in promoting expression of certain MMPs^{33, 34}. In return, MMPs also regulates FN matrix assembly since FN is also a substrate of MMPs³⁵. Even though formation of FN fibrils plays a central role in interacting with cells and other ECM molecules, cell migration is facilitated by a regulated degradation of those fibrils. It is suggested that MT1-MMP degrades FN fibrils and degraded FN is endocytosed with the aid of $\beta 1$ integrin³⁶ (Figure 2B). Thus, under FN regulation, these molecules work in concert to form a unique tumor microenvironment to promote tumor cell migration and invasion.

In addition to interacting with cancer cells, FN, especially EDB-FN, is thought to be involved in regulation of endothelial cells. EDB-FN has been recognized as a biomarker for angiogenesis, the sprouting of new blood vessel from preexisting ones³⁷. By providing oxygen and nutrition to the tumor mass, angiogenesis takes a pivotal part in sustained tumor growth in the primary site, and initiation of new metastasis in distant organs. It has been shown that EDB-FN excreted by cancer cells is able to induce endothelin-1 (ET-1) expression in endothelial cells, which promotes angiogenesis³⁷ (Figure 2B). In turn, EDB-FN upregulation in cancer and endothelial cells is stimulated by ET-1³⁸. This feedback loop augments angiogenesis and cancer progression³⁷. Due to this reason, anti-angiogenic therapy based on silencing EDB-FN expression was developed, which can potentially be used to undermine tumor blood vessel formation³⁹.

1.2 Fibronectin upregulation correlates to cancer malignancy

Clinical evidences indicate that FN, especially onfFN, is overexpressed in various cancer types, including breast cancer^{30, 40}, prostate cancer^{41, 42}, bladder cancer⁴³, oral squamous cell carcinoma⁴⁴, head and neck squamous cell carcinoma⁴⁵, colorectal cancer⁷, and lung cancer⁴⁶. Thus, FN may serve as an omnipresent biomarker regardless of the origins of cancer cells. More importantly, upregulated FN expression is correlated with poor prognosis of the patients. For instance, in studying oral squamous cell carcinoma, Lyons *et al.* reported that strong onfFN expression was seen in 63% and 81% of cases with cervical metastases and extracapsular lymph node spread, respectively⁴⁴. In another study, Young *et al.* evaluated FN expression in invasive breast cancer tissue and a significant correlation was found between FN expression and pathologic tumor stage, pathologic lymph node stage, and histologic grade⁴⁰. A worse survival was also found for the patients with FN expression higher than those with negative expression of FN. Additionally, in a recent study, EDA-FN in urine was demonstrated to be a significant discriminator of bladder cancer patient survival⁴³. All these evidences point towards the value of FN as a biomarker that relates to cancer malignancy and patient survival.

Metastasis, the spread of cells from the primary site of a solid tumor to distant sites, remains the major cause of cancer mortality⁴⁷. Cancer metastasis is a multi-stage process that

includes tumor cells escaping from main tumor mass, invading into blood and lymph system, surviving in circulation, extravasation, and colonization into secondary organs. Metastasis has an early onset in aggressive cancer type, and may occur before the formation of large solid tumors⁴⁸. Disseminated cells are also responsible for recurrence years after dissection of the primary solid tumor⁴⁹. EMT has been thought to play an important role in cancer metastasis¹². During EMT, epithelial cells undergo a transition from a cell-cell contact to a cell-ECM interaction^{50, 51}, allowing mesenchymal cells to reach and squeeze through vessel wall and spread (Figure 2A). In metastatic sites, FN upregulation is one of the earliest events following cancer cell engraftment (Figure 2C). It has been proposed that disseminated cancer cells and metastatic niche in distant organs function in a “seed and soil” manner⁵². This concept is introduced that disseminated tumor cells relies on a receptive microenvironment for outgrowth. Failure of cancer cells to engraft in a hospitable environment would result in tumor sluggish growth or dormancy (Figure 2C). FN overexpression is a common event in metastatic niche^{53, 54}. Surprisingly, this upregulation is found to precede secondary tumor engraftment⁵⁵. FN at metastatic niche can trace back to primary tumors, implying that primary tumor secretes FN as a way to prime certain tissues for tumor engraftment⁵⁶ (Figure 2C). On the other hand, the lack of FN in metastatic niche would lead to decreased metastases formation (Figure 2C). For example, a recent study demonstrated that silencing EDA-FN reduced metastasis of colon cancer cells⁵⁷. In companion with EMT, mesenchymal-to-epithelial transition (MET) is also crucial for metastasis formation. While EMT helps the cancer cells to invade into blood vessel, suppress immune response, and going through extravasation, MET helps in sustained growth of cancer cells in later stage^{58, 59}. However, MET doesn't disqualify FN as a biomarker of cancer metastasis since sustained growth of new solid tumor requires angiogenesis to satisfy its nutrition need. As discussed in previous sections, EDB-FN is a well-known marker for angiogenesis. Together, the upregulation of FN can serve as a marker for localizing cancer metastases.

Cancer drug resistance imposes a major challenge to cancer therapy. It is believed that the generation of cancer stem cells (CSCs), primarily through EMT, is essentially responsible for drug resistance⁶⁰. This endows cancer cells to go through adaptive changes so that they can survive from anticancer therapeutics, including radiation and chemotherapy. Hence, as an EMT marker, FN content can serve as a predictive marker of cancer resistance. High FN expression, as linked to EMT, coincides with loss of epithelial targets such as EGFR and HER2, and emergence of mesenchymal markers⁶⁰. Targeted chemotherapy against these epithelial targets would exert modest or no therapeutic effects in this case. It is also indicated that FN confers drug resistance through protecting cells from apoptosis by activating a number of intracellular signaling pathways^{61–63}. The contribution of β 1-integrin mediated signaling pathway to drug resistance implies the importance of FN-integrin interaction in protecting cancer from chemotherapy⁶⁴. Since FN isoforms, such as EDA- and EDB-FN enhance the FN-integrin interaction, the existence of FN isoforms may compromise the efficacy of chemotherapy and radiation therapy⁶⁵. Indeed, it has been demonstrated that the use of certain chemotherapy drugs, for example Cetuximab, could induce fibronectin biosynthesis, which in turn attenuates its cytotoxicity⁶⁶. In another study, cDNA microarray analysis indicated that the fibronectin-encoding gene, FN1, could be a predictive marker for

resistance to radiation therapy in head and neck squamous cancer⁶⁷. Inspired by this, attempts have been done to counteract this resistance by suppressing EDA-FN expression or function^{68, 69}, which enhances cancer radiosensitivity both in vivo and in vitro. Together, the correlation of FN with cancer resistance may provide a new avenue for predicting therapy response—a crucial step towards personalized therapy.

Understanding the role of FN in cancer is certainly helpful in the design of novel approaches for cancer diagnosis and therapy. Imaging of FN enables the non-invasive detection of cancer-related processes, such as angiogenesis, EMT, metastasis, and cancer resistance, permitting the accurate detection, diagnosis, risk-management of tumors, and non-invasive assessment of therapeutic responses. Therapies directed towards FN can be used for delivery of cytotoxic drugs, cytokines, radioisotopes, and etc. to malignant sites. A novel class of cancer therapeutics can also be developed to reverse FN's tumor-promoting functions by downregulating FN expression, therefore disrupting a number of cancer-promoting processes, such as suffocating oxygen and nutrient supply to tumor through inhibiting angiogenesis, disrupting EMT, and degrading pre-metastatic niche to suppress metastasis. In the following section, we will summarize the advances in developing FN-targeting imaging probes and therapeutic agents and their application in cancer diagnosis and treatment.

2. Targeting Fibronectin for Cancer Imaging

2.1 Upregulated fibronectin as a marker for cancer molecular imaging

In cancer diagnosis, accurate detection, localization, delineation, and risk-stratification of tumors are critical for clinical cancer management and treatment. Cancer diagnostic imaging set force to provide a non-invasive method to fulfill these needs. Cancer diagnostic imaging has seen rapid advances with the evolution of imaging technologies in resolution, speed, and sensitivity⁷⁰. Nevertheless, conventional anatomic imaging methods only rely on morphologic properties or changes for cancer diagnosis. Imaging of the molecular signatures of cancer has the ability to provide biochemical information for more accurate characterization and diagnosis. Substantial progresses have been made in developing contrast agents and probes for molecular imaging of cancer biomarkers and elucidating cellular or subcellular events non-invasively⁷⁰.

Biopsy is currently the gold-standard method for cancer detection and risk-stratification. But biopsy only examines limited sample regions in possible disease sites. Taking prostate cancer for example, even though saturation biopsy is used routinely for prostate cancer evaluation, the overall sensitivity and specificity with prostate biopsy are still very low, approximately 32% and 51%, respectively^{71, 72}. In addition, as an invasive approach, biopsy is associated with bleeding, pain, anxiety, possible infections, and other unintended side effects. Molecular imaging is a non-invasive approach that can probe biomarker expression related to the tumor malignancy throughout the entire regions of interest. Therefore, molecular imaging can provide more accurate detection and diagnosis of cancer based on complete characterization of the biomarker expression, facilitating decision-making in the intervention and management of the disease.

FN has been tested as a biomarker for molecular imaging. Its abundant expression in the ECM of malignant cancer presents excellent accessibility of imaging probes to the molecular target for effective molecular imaging. Antibodies and peptides have been developed to target FN and its isoforms.

Table 1 summarizes some of the reported targeting ligands and their applications in cancer imaging and therapy. Majority of these ligands have been developed to target onFN because of specific high expression of the biomarker in cancer.

Antibodies for onFN isoforms were reported in early 1990s. EDB-FN targeting antibodies, such as BC-1, are generated by mice immunization with EDB-FN^{107, 108}. Their epitopes are on another FNIII domain unmasked by EDB insertion¹⁰⁹. Phage display against bacteria expressed EDB protein from human scFv antibody library resulted in another EDB-specific antibody, named L19¹¹⁰. Several forms of antibodies containing the variable region of L19(scFv) were later derived, including L19(scFv)₂, L19SIP (SIP: small immunoprotein), AP39 (complete IgG1)¹¹¹, and L19-His. L19SIP shows a better plasma stability, pharmacokinetics, and tumor accumulation (2–5 times increase over L19(scFv))¹¹¹, and has been frequently used to construct imaging or therapeutic agents. AP39 and L19(scFv)₂ have also been labeled with radionuclide for imaging or therapy purposes¹¹¹. An antibody scFv named F8 against EDA-FN, identified using colony filtering screening, has also been tested for cancer targeting¹¹².

Small peptides have been identified to target onFN and FibFN in cancer. Small peptides are advantageous in low immunogenicity, versatility in chemical modification, and cost-effective production as compared to antibodies. Small peptides also possess rapid extravasation and high tissue penetrating ability in tumor targeting¹¹³. This enables them to target not only vascular FN, but also FN matrix surrounding cancer cells. An EDB binding scaffold-like peptide, APT_{EDB}, is devised with phage display technology¹¹⁴. APT_{EDB} consists of a stabilizing scaffold and two target-binding regions. Taking advantage of the three-dimensional structure for optimal binding, APT_{EDB} exhibited a high binding affinity (65 nM) to EDB protein. A small cyclic nonapeptide ZD2 of the sequence of CTVRTSADC was recently identified using peptide phage display to target EDB. This peptide demonstrated excellent specific targeting to tumor in vivo¹⁰¹. Another class of FN-targeting ligands is the peptides that target fibronectin-fibrin complexes. Cyclic peptides, CGLIIQKNEC (CLT1) and CNAGESSKNC (CLT2), and pentapeptide CREKA identified from phage display exhibit specific binding to FibFN in tumor stroma¹¹⁵.

These targeting agents have been used in the preparation of imaging agents targeting FN and its isoforms for cancer imaging. The effectiveness of the agents has been demonstrated in various tumor models. Some of the agents have been tested in human patients. Recent advances in molecular imaging of FN and onFN are highlighted in the following section.

2.2 Nuclear imaging

Nuclear imaging is a highly sensitive molecular imaging modality and provides detection, localization, and quantification of biomarkers in cancer imaging. Radioisotopes labeled with targeting ligands are commonly used as probes in nuclear imaging. Images of biomarker

localization are acquired by recording the γ -rays emitted from the radionuclides of the imaging probes on gamma cameras. Depending on dimensions of acquired image, nuclear imaging can be classified into gamma-ray scintigraphy, which produces two-dimensional images, and single-photon emission computed tomography (SPECT) and positron emission tomography (PET), which produce three-dimensional images.

The probes for nuclear imaging are often developed by chemical coupling of γ -ray emitting radionuclides with a short half-life to targeting ligands. The pharmacokinetics of the targeting agents and radionuclide half-lives should be considered in the design of the imaging probes for optimal detecting sensitivity. Antibodies with a larger size possess a relatively long pharmacokinetic half-life. A longer time is needed for the clearance of the antibodies from the circulation and background tissues for effective image contrast. In this case, radioisotopes with long half-lives, such as ^{99m}Tc , ^{123}I , ^{76}Br , ^{124}I with $t_{1/2} = 6, 13, 16.2$ h, and 4.18 d, respectively, are often coupled with antibodies. Small peptides normally exhibit relatively fast target binding and accumulation, and fast clearance from the circulation and background tissue. Therefore, the pharmacokinetic half-life of peptides, rather than the radionuclide half-life, is a major factor in the design of peptide radioisotope probes.

The potential of molecular imaging of EDB-FN with a radioactive probe in cancer imaging was first demonstrated with BC-1 antibody⁸⁸. BC-1 antibody was labeled with ^{99m}Tc for gamma scintigraphy and SPECT⁸⁸. The preliminary study of the probe ^{99m}Tc -BC-1 in 5 brain cancer patients showed specific tumor uptake and very low nonspecific uptake in the bone marrow, liver and spleen. The probe provided a more accurate tumor detection than nonspecific indicator, ^{99m}Tc -DTPA, and its tumor uptake strongly correlated with specific oncofetal fibronectin expression.

Significant progress has been made on molecular imaging of EDB-FN using L19 antibody and its derivatives. In a clinical study, L19(scFv)₂ antibody labeled with ^{123}I , ^{123}I -L19(scFv)₂, was tested in detecting multiple cancers, including brain, lung and colorectal cancer with immunoscintigraphy⁷³. Sixteen out of 20 patients injected with ^{123}I -L19(scFv)₂ showed positive cancer detection, while the 4 patients with negative scans had tumors that did not express EDB-FN. In another study, the L19(scFv) variant, AP39, was labeled with ^{99m}Tc for imaging F9 teratocarcinoma. ^{99m}Tc -AP39 showed favorable pharmacokinetic and tumor-targeting properties with low radioactivity in the blood. The probe also demonstrated rapid renal excretion and high *in vivo* stability⁸⁴. L19SIP was also labeled with ^{76}Br for a small animal PET imaging⁸⁶. Although this probe demonstrated fast and specific tumor targeting, a major concern arose due to the slow renal clearance of this probe. Persistent radioactivity in blood and stomach suggests partial ^{76}Br -L19SIP debromination *in vivo*, which led to lower target to non-target ratios. Later, ^{124}I -L19SIP was synthesized and tested for PET tumor imaging in a FaDu head and neck cancer model, in which a clear delineation of tumors as small as 50 mm³ was achieved⁷⁹. Due to similar pharmacokinetics of ^{124}I -L19SIP and ^{131}I -L19SIP, PET with ^{124}I -L19SIP was used to predict proper dose of ^{131}I -L19SIP for immunotherapy in patients with brain metastasis to achieve the optimal delivery of radiation to the tumor while minimizing burden to the dose-limiting organs (bone red marrow and normal brain)⁸⁰. More recently, ^{131}I -L19SIP was

tested in a prostate cancer patient with 2D-scintigraphy, as highlighted in Figure 3. A selective uptake of ^{131}I -L19SIP was seen in metastatic prostate tumors, indicating EDB-FN as a promising target in prostate cancer⁸².

There has been no report on using FN-targeting peptides for PET or SPECT detection of cancer. Small peptides are advantages over antibodies due to their rapid tumor accumulation and fast clearance in circulation and background. In this regard, high tumor-to-background ratio at earlier time points after injection can be achieved in nuclear imaging using radiolabeled peptides. Thus far, several small peptides have been conjugated to paramagnetic chelates to develop targeted MRI contrast agents^{90–92} (see later). In fact, the peptide ligand conjugates can be readily radiolabeled with radioisotopes, such as ^{55}Co , ^{64}Cu , ^{67}Cu , ^{47}Sc , ^{68}Ga , $^{99\text{m}}\text{Tc}$, and etc., for PET or SPECT imaging. In addition, these peptides can also be labeled with ^{18}F for PET^{116, 117}.

2.3 Magnetic resonance imaging

Magnetic resonance imaging (MRI) offers higher spatial resolution images of soft tissues and presents no ionizing radiation to patients. The challenge with MRI is its inherently low sensitivity in molecular imaging. However, effective MR molecular imaging of cancer can still be achieved by targeting highly upregulated FN in tumor ECM, which will allow specific binding of sufficient targeted contrast agents to generate detectable MR signal. Despite the success of nuclear imaging using EDB-FN targeting antibodies, antibodies with large size may not be suitable for targeted MRI contrast agents, especially for gadolinium-based contrast agents, because they cannot be rapidly excreted after the diagnostic imaging, exposing patients to potential toxic effects. In contrast, small molecular targeted contrast agents developed with small peptides are desired due to their rapid extravasation and accumulation in tumor tissues, and fast clearance of unbound agent from the circulation.

Small peptide targeted MRI contrast agents have been constructed by conjugating Gd chelates to FibFN-targeting peptides for cancer imaging^{95, 118, 119}. CLT1-(Gd-DTPA) exhibited significant tumor contrast enhancement for at least 60 min post injection in HT-29 human colon carcinoma xenografts (Figure 4A)⁹³. This agent was also effective for imaging of MDA-MB-231 breast carcinoma in a mouse model¹²⁰, resulting in significant tumor contrast enhancement at a dose of 0.05 mmol/kg for at least 60 min after injection. In another study, the macrocyclic Gd chelate, Gd-DOTA, was also conjugated to CLT1 peptide. Macrocyclic chelate Gd-DOTA and its derivatives have higher kinetic stability than Gd-DTPA against transmetallation and more complete excretion from the body. Multiple peptide molecules and chelates were conjugated onto a generation 2 dendrimeric nanoglobule to give CLT1-G2-(Gd-DOTA) and to improve the efficiency of targeting and contrast enhancement in MR molecular imaging. The nanoglobular agent contains 3 CLT1 peptides and 20 Gd-DOTA chelates on average, and has high T_1 and T_2 relaxivities of 11.6 and 15.7 $\text{mM}^{-1}\text{s}^{-1}$ per Gd at 1.5T, respectively (Figure 4B)⁹⁵. It produced significant tumor contrast enhancement up to 50 min post-injection in a mouse orthotopic PC3 prostate tumor model. A smaller targeted contrast agent with one CLT1 peptide and 4 Gd-DOTA chelates CLT1-dL-(Gd-DOTA)₄ was synthesized by conjugating the Gd-DOTA monoamide chelates to the CLT1 peptide via generation 1 lysine dendrimer to reduce the size of the targeted contrast

agent and to facilitate rapid excretion after imaging (Figure 4C)^{121–123}. Similarly, CLT1-dL-(Gd-DOTA)₄ demonstrated a high T₁ relaxivity (10.1 mM⁻¹s⁻¹ per Gd) and significant tumor contrast enhancement in orthotopic PC3 human prostate cancer model at a low dose of 0.03 mmol Gd/kg. CLT1-dL-(Gd-DOTA)₄ showed rapid renal clearance of the unbound agent and very low Gd accumulation in normal organs at 48 h after injection. Using the same approach, CREKA-dL-Gd(DOTA)₄ was constructed and tested for prostate cancer imaging⁹³. CREKA peptide and its targeted contrast agents exhibited better water solubility than CLT1 peptide and targeted contrast agents. A tripod macrocyclic Gd(III) chelate CREKA-Tris-Gd(DOTA)₃ was also synthesized and tested for breast cancer imaging (Figure 4D)¹¹⁹. Specific targeting of this agent to FibFN in tumor microenvironment resulted in greater contrast enhancement than commercialized contrast agent ProHance[®]. A rapid clearance of the contrast agents via renal filtration was seen, resulting in a low tissue retention.

Since FN is highly expressed in the metastatic niches, contrast enhanced MRI has a potential to image micrometastases and very small tumors in high spatial resolution by targeting the highly expressed FN with a targeted contrast agent. Zhou et al. recently demonstrated that CREKA-Tris(Gd-DOTA)₃ was able to detect micrometastases of breast cancer in animal models⁹⁶. As shown in this study, metastatic tumors had much higher FN expression than the primary tumor, enabling sufficient binding of the contrast agent in micrometastases for sensitive detection. By co-registering detected micrometastases in MRI with high-resolution fluorescence cryoimaging of the fluorescently labeled tumors, MRI with CREKA-Tris(Gd-DOTA)₃ was shown to detect micrometastases with size <0.5 mm in diameter at a sensitivity of 83%, extending the cancer detection limit of the current clinical imaging modalities. The targeted contrast agent has shown the potential to facilitate early detection of high-risk breast cancer and micrometastases so that early treatment is possible.

Besides Gd-based contrast agents, FN-targeting peptides, including CREKA and APT_{E_{DB}}, have also been used to modify super paramagnetic iron oxide nanoparticles (SPIO) for T₂*-weighted MR molecular imaging^{98, 99, 103}. It has been shown that CREKA-SPIO could induce additional plasma clotting in tumor, producing binding sites for more nanoparticles. This clotting-based amplification greatly enhanced tumor imaging^{98, 99, 103}. Preparation of the APT_{E_{DB}} labeled SPION nanoparticles is depicted in Figure 6. APT_{E_{DB}}-TCL-SPIO nanoparticles showed significant accumulation in breast tumor initiating cells, NDY-1, with specific overexpression of EDB-FN. In contrast, APT_{E_{DB}}-TCL-SPIO, could not bind to non-breast tumor initiating cells, such MCF-7 cells, which had low EDB-FN expression¹⁰³.

2.4 Other imaging modalities

FN-targeting antibodies and peptides can be readily modified with fluorescent dyes for optical imaging. Even though limited studies have been done with a specific focus on FN-targeting optical imaging probe for in vivo cancer imaging^{101, 125}, FN-targeting fluorescent probes have been developed in most studies for validating tumor targeting efficiency of the ligands. The probes also have been tested for in vivo diagnosis of other diseases, including rheumatoid arthritis, atherosclerosis, etc.^{126–128}. The limitation of optical imaging is the penetration of light in tissues. However, there is an increasing need for optical imaging

probes in delineation of tumor margin during surgery. FN-targeting optical imaging probes could be used in image-guided dissection of tumors, meanwhile minimizing harm to healthy tissue.

3. Targeting fibronectin in cancer therapy

3.1 FN targeting radiotherapy

Cancer therapy can be achieved by replacing the γ -emitters in FN targeting imaging probes with therapeutic radioisotopes. This strategy embraces the benefit of selective targeting and decreased systemic toxicity. The first reported FN targeting radiation therapy was ^{125}I labeled BC-1 antibody (named as ^{125}I -BC-1), which accumulated favorably in human tumor implants⁸⁹. Later studies directed towards using L19SIP antibody due to its specific targeting to EDB domain. Administration of ^{131}I -L19SIP resulted in selective uptake in SW1222 and LS174T colorectal tumors, which led to tumor growth retardation and prolonged survival of mice⁸⁵. ^{131}I -L19SIP was also tested in treating FaDu and HNX-OE head and neck squamous cell carcinoma (HNSCC) model¹²⁹. A combination of ^{131}I -L19SIP and anti-EGFR mAb cetuximab achieved a significant therapeutic effect in imaging and treating Hodgkin and non-Hodgkin lymphoma patients¹³⁰. ^{131}I -L19SIP radioimmunotherapy induced a sustained partial response in 2 relapsed Hodgkin lymphoma patients. Despite these promising results, the hematologic toxicity caused by the high and long-lasting radioactivity of radiolabeled antibodies in the blood is still a limiting factor. The continuous non-specific radiation is particularly harmful to highly radiosensitive red marrow. In an attempt to further minimize the systemic toxicity and enhance the therapeutic effect, the pre-targeting strategy has been integrated in EDB-FN-targeted radiotherapy of glioblastoma¹³¹. This study used a bispecific antibody, AP39xm679, prepared by coupling anti-EDB antibody AP39 and histamine-succinyl-glycine (HSG) antibody m679. In this strategy, AP39xm679 was first administered and the ^{111}In -labeled HSG-DOTA complex then was injected when the bispecific antibody reaches maximum in tumor and sufficient clearance in normal tissue (around 25 or 41 hours after bispecific antibody injection). With a strong affinity to pretargeted bispecific antibody in tumor, small radiolabeled compound would quickly extravasate, diffuse, and bind to previously administered target in the tumor, meanwhile unbound molecules underwent rapid clearance. Compared with ^{125}I -L19SIP, the tumor uptake of the pretargeted ^{111}In -carrying peptide was significant higher over 7 days, and could lead to at least 3 folds increase in therapeutic efficacy¹³¹.

3.2 Targeted delivery of anti-tumor agents

FN-targeting ligands have been used to deliver chemotherapeutics to FN expressing tumors. Targeted delivery of these cytotoxic drugs to tumor could make the best use of the drug's anti-tumor effect, while minimizing harm to normal cells. APT_{EDB} was conjugated to doxorubicin (DOX)-containing liposomes for targeted drug delivery (Figure 7). As reported, APT_{EDB} targeted liposomes specifically accumulates in glioma, resulting in 55% decrease in tumor size as compared to 20% decrease with free doxorubicin¹⁰⁴. APT_{EDB} was also tested in guiding PEG-PLA nanoparticles loaded with paclitaxel (PTX) for treating glioma⁹⁴. The EDB targeting nanoparticles loaded with PTX resulted in enhanced tumor regression and a prolonged survival as compared to the free drug. Direct conjugation of APT_{EDB} to docetaxel

(DTX) also yielded an improved delivery efficiency of docetaxel in glioma, with enhanced therapeutic effects¹⁰⁵. In another study, ZD2 was conjugated to DOX, yielding an amphiphilic compound that self-assembles into nanoparticles¹⁰². These nanoparticles targeted efficiently to solid PC3 tumors, and disassembled in the high thiol environment in tumor to release DOX. As a result, an enhanced tumor-inhibiting effect was achieved. CLT1 was used to modify PEG-PLA nanoparticles to delivery PTX to glioma¹³². By targeting overexpressed FibFN in tumor, the CLT1 modified PTX-loaded nanoparticles exhibited favorable nanoparticle penetration into the core of glioma spheroid and therefore induced more inhibitive effects on glioma growth. Similarly, CREKA was recently used to modify polyamidoamine (PAMAM) dendrimer¹⁰⁰. The modified dendrimer was able to penetrate glioblastoma (GBM) tissue and enhance the retention effect, which could be potentially used to deliver chemotherapy drugs.

FN-targeting ligands have also been used for targeted delivery of cytokines, including interleukin-2 (IL-2), interleukin-12 (IL-12), and TNF α . Cytokines are able to activate a wide range of immunological cells, including cytotoxic T cells and natural killer cells. However, therapeutic efficacy of cytokines is limited by its short blood half-life and severe toxicity related to vascular leak syndrome at high doses. The genetic fusion of scFv L19 and IL-2 resulted in L19-IL-2, which enabled specific delivery of IL-2 to F9 murine teratocarcinoma so that an efficacious concentration can be achieved in tumor without causing severe systemic toxicity⁷⁴. Concomitant with inhibited tumor growth, tumors treated with L19-IL2 had high accumulation of CD8+ cytotoxic T lymphocytes, CD4+ cells, CD11b+ cells (macrophages and natural killer cells), symphonizing with the function of IL2⁷⁴. Besides, L19-IL-2 has been tested in preclinical studies to treat other types of cancers, including lymphoma⁷⁵ and pancreatic cancer⁷⁶, in which L19-IL2 consistently showed enhanced therapeutic potency. L19-IL2 is branded as DARLEUKIN[®] for clinical use, and is mainly used to treat melanoma, head and neck cancer, and lymphoma in combination with L19-TNF, dacarbazine or rituximab. Recent phase II clinical evaluation of L19-IL2 in treating melanoma patients showed a promising result in terms of reducing metastasis and extending patient survival^{77, 78}. The combined treatment of L19-IL2 and dacarbazine was reasonably tolerated, and all side effects encountered in the study were manageable and reversible. Similarly, an EDA-FN targeting antibody, F8, was used to deliver IL-2 to a variety of cancers, including renal cell carcinoma⁹⁰, melanoma⁹¹, colon cancer, lymphoma, and teratocarcinoma⁹². L19 was also used to modify IL-12, yielding L19-IL-12, to treat mouse lung metastases and aggressive murine tumors⁸¹. Enhanced anti-tumor effect was seen with the increased tumor infiltration with lymphocytes, macrophages, and natural killer cells. Humanized BC-1 antibody, huBC1, was also developed to modify IL-12 for tumor therapy¹⁰⁴. One cycle of treatment with huBC1-IL12 resulted in tumor suppression in PC3mm2 (human prostate cancer), A431 (human melanoma), and HT29 (human colon cancer) subcutaneous tumor models, and PC3mm2 lung metastasis model¹⁰⁴. A phase I clinical study was conducted using huBC1-IL12, and demonstrated that huBC1-IL12 was well tolerated at the dose of 15 μ g/kg weekly. Stable disease was seen in 46% of the patients^{133, 134}.

Tumor necrosis factor (TNF) is another cancer-related cytokine modified with FN-targeting strategies. An antibody-cytokine fusion of L19 and TNF, L19-TNF, was constructed for

cancer therapy. Initial effort with L19-TNF therapy in murine models induced a retardation of tumor growth, but no curative effect was observed¹³⁵. However, the combination of L19-IL2 and L19-TNF therapy showed a synergetic effect to eradicate F9 teratocarcinomas grafted in immunocompetent mice¹³⁶. Also, tumor development was delayed when the cured mice were again challenged with tumor cells, indicating an induction of anti-tumor vaccination effect of the combination therapy. Treatment with L19-TNF in combination with melphalan induced tumor regression and long lasting tumor rejection in 83% of BALB/c mice with WEHI-164 fibrosarcoma and 33% of animals with C51 colon carcinoma⁸³. Similar results were seen for treatment of sarcomas and melanoma^{137, 138}. Encouraged by these preclinical trials, a phase I/II first-in-human trial was conducted with L19-TNF monotherapy. Dose escalation clinical trials showed little toxic effects in patients with solid metastatic cancers in the dose range of 1.3–14 µg/kg¹³⁹. In another study, L19-TNF was tested in treating melanoma patients¹⁴⁰. With only 6.25% of the dose approved for TNF, L19-TNF induced objective responses in 89% of patients, including a complete response in 5/10 patients. The response was durable at 12 months in four patients. Recently, results on a phase II study that evaluated effects of L19-IL2/L19-TNF combination therapy on stage II or stage IV M1a melanoma patients were reported¹⁴¹. In this study, intralesional administration of L19-IL2 and L19-TNF resulted in complete responses in 32 melanoma lesions in 20 efficacy-evaluated patients, with only mild side effects limited to injection site reactions. This intralesional administration of L19-IL2 and L19-TNF is a simple and effective method for local control of inoperable melanoma lesions. Currently, this approach has been approved by German and Italian authorities for the phase III clinical trial.

Considering the role of onfFN in cancer, attempts have been made to silence the expression of onfFN in vivo for cancer therapy. One approach toward suppressing onfFN expression is RNA interference (RNAi)^{37, 39, 142}. RNAi therapy requires safe and efficient delivery of siRNA to tumor sites with high onfFN expression. Advances in developing siRNA delivery systems made this a possibility^{143, 144}. Studies have been done using APT_{EDB} as targeting moiety, with EDB siRNA encapsulated in liposome for treatment of a high-risk breast cancer model derived from breast cancer stem cells (BCSC), as illustrated in Figure 7. This design enabled simultaneous EDB-FN targeting and siRNA therapy for BCSC tumors with high EDB-FN expression¹⁰⁶.

3.3 Cancer vaccination against FN

The field of cancer vaccine research has expanded rapidly in recent years, and a major focus has been on the self-antigen vaccination approach, which entails eliciting immune response to control and treat cancer¹⁴⁵. As important cancer markers in tumor ECM, EDA and EDB domains have been used as targets for cancer vaccination. A vaccine was developed against EDB-FN, which elicited production of anti-EDB antibodies and resulted in a 70% tumor volume reduction in T241 fibrosarcoma tumor model¹⁴⁶. Vaccination against EDA showed that it could attenuate the progression of metastatic breast cancer¹⁴⁷. This observation was accompanied by reduction of primary tumor growth in MMTV-PyMT transgenic model, with enhanced recruitment of immune cells and disruption of tumor blood vessel. Compared with monoclonal antibodies, which require repeated and long-term administration, the low cost and long-lasting effect of vaccination makes this approach favorable. Recently, Ahn et

al. reported the use of EDB-carrying gold nanoparticles (AuNPs) as vaccines for immunotherapy of breast cancer¹⁴⁸. This AuNP-based antigen delivery system induced humoral and cellular immunity against EDB-FN. The characteristics of AuNPs, including chemical inertness, controllable size, and enhanced uptake by dendritic cells (DCs), make it a promising platform for cancer immunotherapy. The use of cancer vaccine against EDA and EDB has yet to be tested for clinical use. Possible side effect for vaccination using EDA and EDB as antigen must be considered, because EDA and EDB expression is also prevalent in wound healing and the female menstrual cycle, which may be affected by endogenous antibodies directed towards the EDA and EDB domains.

3.4 FN targeting photodynamic and photothermal therapy

Photodynamic and photothermal therapy are alternative tumor-ablative and function-sparing oncologic intervention approaches. Activation of a tumor-localizing photothermal agent or photosensitizer (PS) by local illumination of tumor with light of a specific wavelength the photothermal agents or PS can induce cytotoxicity¹⁴⁹. In photodynamic therapy, the excited PS transfers its energy to molecular oxygen, thus generating cytotoxic reactive oxygen species (ROS) that can oxidize key cellular macromolecules leading to tumor cell death. Unlike drug delivery systems that carry toxic anti-cancer cargos, this system is entirely non-toxic until activated in tumors. Efficient delivery of PS to cancer is critical for optimal tumor photodynamic and photothermal therapy. L19 antibody was conjugated to a photosensitizer bis(triethanolamine)Sn(IV) chlorin e_6 to give a targeted PS SnChe₆-(SIP)L19⁸⁷. After intravenous injection of this EDB-FN targeting PS and NIR activation, an arrest of tumor growth was observed in mice, along with complete tumor blood vessel occlusion or damage. Therefore, by targeting EDB-FN, this photodynamic therapy can serve as a novel approach for cancer therapy.

CRKEA peptide was conjugated to multi-wall nanotubes (MWNTs) via PEG for photothermal therapy of A549 human lung cancer model⁹⁷. MWNTs are near-infrared radiation (NIR) absorbing materials with the ability of photothermal tumor ablation. Mediated by CREKA peptide that targets FibFN, the nanoparticles were able to elevate temperature specifically in the tumor region under NIR illumination. With four times of illumination, the CMWNTs-PEG almost totally eradicated the tumor xenografts. This novel method for cancer therapy could be expanded using other FN-targeting ligands. Further evaluation of biocompatibility of the nanotubes is necessary to advance the therapy into clinics.

4. Conclusions

FN and its isoforms play a significant role in cancer biology and are promising targets of cancer imaging and therapy. Antibodies and small peptides have been developed to target upregulated FN and its isoforms in malignant cancer to deliver imaging agents and therapeutics for cancer detection and therapy. Imaging probes and contrast agents have been developed based on these ligands showing the promise for cancer molecular imaging in preclinical and clinical studies. FN-targeting antibodies and peptides have been tested for delivery of radioisotopes, chemotherapeutics, and cytokines for cancer therapy. Some of FN-

targeting imaging agents and therapeutics have progressed into various stages of clinical development. The imaging agents and therapeutics targeting overexpressed FN in cancer have the potential to improve the accuracy for early detection and diagnosis of malignant tumor and to enhance the efficacy of cancer therapies.

Acknowledgments

This research was supported in part by the NIH grant R01 CA194518. The authors thank Ms. Nadia Ayat for proofreading of the manuscript.

References

1. Mao Y, Keller ET, Garfield DH, Shen K, Wang J. *Cancer Metastasis Rev.* 2013; 32:303–315. [PubMed: 23114846]
2. Joyce JA, Pollard JW. *Nat Rev Cancer.* 2009; 9:239–252. [PubMed: 19279573]
3. Zhou Z, Lu ZR. *Adv Drug Deliver Rev.* 2016
4. Kumra H, Reinhardt DP. *Adv Drug Deliver Rev.* 2016; 97:101–110.
5. Hynes RO, Yamada KM. *J Cell Biol.* 1982; 95:369–377. [PubMed: 6128348]
6. Sottile J, Hocking DC. *Molecular biology of the cell.* 2002; 13:3546–3559. [PubMed: 12388756]
7. Inufusa H, Nakamura M, Adachi T, Nakatani Y, Shindo K, Yasutomi M, Matsuura H. *Cancer.* 1995; 75:2802–2808. [PubMed: 7773930]
8. Fukuda T, Yoshida N, Kataoka Y, Manabe R, Mizuno-Horikawa Y, Sato M, Kuriyama K, Yasui N, Sekiguchi K. *Cancer Res.* 2002; 62:5603–5610. [PubMed: 12359774]
9. Tan MH, Sun Z, Opitz SL, Schmidt TE, Peters JH, George EL. *Blood.* 2004; 104:11–18. [PubMed: 14976060]
10. Astrof S, Crowley D, Hynes RO. *Developmental biology.* 2007; 311:11–24. [PubMed: 17706958]
11. Wierzbicka-Patynowski I, Schwarzbauer JE. *J Cell Sci.* 2003; 116:3269–3276. [PubMed: 12857786]
12. Mani SA, Guo W, Liao MJ, Eaton EN, Ayyanan A, Zhou AY, Brooks M, Reinhard F, Zhang CC, Shipitsin M, Campbell LL, Polyak K, Brisken C, Yang J, Weinberg RA. *Cell.* 2008; 133:704–715. [PubMed: 18485877]
13. Christofori G. *Nature.* 2006; 441:444–450. [PubMed: 16724056]
14. Ding Y, Gelfenbeyn K, Freire-de-Lima L, Handa K, Hakomori SI. *Febs Lett.* 2012; 586:1813–1820. [PubMed: 22641031]
15. Park J, Schwarzbauer JE. *Oncogene.* 2014; 33:1649–1657. [PubMed: 23624917]
16. Johansson S, Svineng G, Wennerberg K, Armulik A, Lohikangas L. *Front Biosci.* 1997; 2:d126–146. [PubMed: 9159220]
17. Redick SD, Settles DL, Briscoe G, Erickson HP. *J Cell Biol.* 2000; 149:521–527. [PubMed: 10769040]
18. Schiefner A, Gebauer M, Skerra A. *J Biol Chem.* 2012; 287:17578–17588. [PubMed: 22442152]
19. Mao Y, Schwarzbauer JE. *Matrix biology : journal of the International Society for Matrix Biology.* 2005; 24:389–399. [PubMed: 16061370]
20. Manabe R, Ohe N, Maeda T, Fukuda T, Sekiguchi K. *J Cell Biol.* 1997; 139:295–307. [PubMed: 9314547]
21. Xia P, Culp LA. *Exp Cell Res.* 1994; 213:253–265. [PubMed: 8020597]
22. Liao YF, Gotwals PJ, Koteliansky VE, Sheppard D, Van De Water L. *J Biol Chem.* 2002; 277:14467–14474. [PubMed: 11839764]
23. Chen W, Culp LA. *Clinical & experimental metastasis.* 1998; 16:30–42. [PubMed: 9502075]
24. Clark RA, Lanigan JM, DellaPelle P, Manseau E, Dvorak HF, Colvin RB. *J Invest Dermatol.* 1982; 79:264–269. [PubMed: 6752288]
25. Zerlauth G, Wolf G. *Am J Med.* 1984; 77:685–689. [PubMed: 6385694]

26. Choate JJ, Mosher DF. *Cancer*. 1983; 51:1142–1147. [PubMed: 6571802]
27. Wilhelm O, Hafter R, Coppenrath E, Pflanz MA, Schmitt M, Babic R, Linke R, Gossner W, Graeff H. *Cancer Res*. 1988; 48:3507–3514. [PubMed: 3130986]
28. Malik G, Knowles LM, Dhir R, Xu S, Yang S, Ruoslahti E, Pilch J. *Cancer Res*. 2010; 70:4327–4334. [PubMed: 20501851]
29. Chen P, Cescon M, Bonaldo P. *Trends in molecular medicine*. 2013; 19:410–417. [PubMed: 23639582]
30. Ioachim E, Charchanti A, Briasoulis E, Karavasilis V, Tsanou H, Arvanitis DL, Agnantis NJ, Pavlidis N. *Eur J Cancer*. 2002; 38:2362–2370. [PubMed: 12460779]
31. Sottile J, Shi F, Rublyevska I, Chiang HY, Lust J, Chandler J. *Am J Physiol Cell Physiol*. 2007; 293:C1934–1946. [PubMed: 17928541]
32. Erat MC, Slatter DA, Lowe ED, Millard CJ, Farndale RW, Campbell ID, Vakonakis I. *Proc Natl Acad Sci U S A*. 2009; 106:4195–4200. [PubMed: 19251642]
33. Okamura Y, Watari M, Jerud ES, Young DW, Ishizaka ST, Rose J, Chow JC, Strauss JF 3rd. *J Biol Chem*. 2001; 276:10229–10233. [PubMed: 11150311]
34. Saito S, Yamaji N, Yasunaga K, Saito T, Matsumoto S, Katoh M, Kobayashi S, Masuho Y. *J Biol Chem*. 1999; 274:30756–30763. [PubMed: 10521465]
35. Takino T, Yoshimoto T, Nakada M, Li Z, Domoto T, Kawashiri S, Sato H. *Biochem Biophys Res Commun*. 2014; 450:1016–1020. [PubMed: 24976399]
36. Shi F, Sottile J. *J Cell Sci*. 2011; 124:4039–4050. [PubMed: 22159414]
37. Khan ZA, Chan BM, Uniyal S, Barbin YP, Farhangkhomee H, Chen S, Chakrabarti S. *Angiogenesis*. 2005; 8:183–196. [PubMed: 16308732]
38. Marini M, Carpi S, Bellini A, Patalano F, Mattoli S. *Biochem Biophys Res Commun*. 1996; 220:896–899. [PubMed: 8607863]
39. Cseh B, Samantha F-S, Grall Dominique, et al. *JOURNAL OF CELL SCIENCE*. 2010; 123:3989–3999. [PubMed: 20980391]
40. Bae YK, Kim A, Kim MK, Choi JE, Kang SH, Lee SJ. *Hum Pathol*. 2013; 44:2028–2037. [PubMed: 23684510]
41. Suer S, Sonmez H, Karaaslan I, Baloglu H, Kokoglu E. *Cancer Lett*. 1996; 99:135–137. [PubMed: 8616816]
42. Albrecht M, Renneberg H, Wennemuth G, Moschler O, Janssen M, Aumuller G, Konrad L. *Histochem Cell Biol*. 1999; 112:51–61. [PubMed: 10461812]
43. Arnold SA, Loomans HA, Ketova T, Andl CD, Clark PE, Zijlstra A. *Clin Exp Metastasis*. 2016; 33:29–44. [PubMed: 26456754]
44. Lyons AJ, Bateman AC, Spedding A, Primrose JN, Mandel U. *The British journal of oral & maxillofacial surgery*. 2001; 39:471–477. [PubMed: 11735145]
45. Mhaweck P, Dulguerov P, Assaly M, Ares C, Allal AS. *Oral oncology*. 2005; 41:82–88. [PubMed: 15598590]
46. Khan ZA, Caurtero J, Barbin YP, Chan BM, Uniyal S, Chakrabarti S. *Experimental lung research*. 2005; 31:701–711. [PubMed: 16203624]
47. van Denderen BJ, Thompson EW. *Nature*. 2013; 493:487–488. [PubMed: 23344357]
48. Husemann Y, Geigl JB, Schubert F, Musiani P, Meyer M, Burghart E, Forni G, Eils R, Fehm T, Riethmuller G, Klein CA. *Cancer Cell*. 2008; 13:58–68. [PubMed: 18167340]
49. Rice J. *Nature*. 2012; 485:S55–57. [PubMed: 22648500]
50. Kalluri R, Weinberg RA. *J Clin Invest*. 2009; 119:1420–1428. [PubMed: 19487818]
51. Kalluri R. *J Clin Invest*. 2009; 119:1417–1419. [PubMed: 19487817]
52. Psaila B, Lyden D. *Nat Rev Cancer*. 2009; 9:285–293. [PubMed: 19308068]
53. Rybak JN, Roesli C, Kaspar M, Villa A, Neri D. *Cancer Res*. 2007; 67:10948–10957. [PubMed: 18006840]
54. Mastarone DJ, Harrison VS, Eckermann AL, Parigi G, Luchinat C, Meade TJ. *J Am Chem Soc*. 2011; 133:5329–5337. [PubMed: 21413801]

55. Kaplan RN, Riba RD, Zacharoulis S, Bramley AH, Vincent L, Costa C, MacDonald DD, Jin DK, Shido K, Kerns SA, Zhu Z, Hicklin D, Wu Y, Port JL, Altorki N, Port ER, Ruggero D, Shmelkov SV, Jensen KK, Rafii S, Lyden D. *Nature*. 2005; 438:820–827. [PubMed: 16341007]
56. Erler JT, Bennewith KL, Cox TR, Lang G, Bird D, Koong A, Le QT, Giaccia AJ. *Cancer Cell*. 2009; 15:35–44. [PubMed: 19111879]
57. Ou J, Deng J, Wei X, Xie G, Zhou R, Yu L, Liang H. *Stem cell research*. 2013; 11:820–833. [PubMed: 23811539]
58. Hugo H, Ackland ML, Blick T, Lawrence MG, Clements JA, Williams ED, Thompson EW. *J Cell Physiol*. 2007; 213:374–383. [PubMed: 17680632]
59. Malanchi I, Santamaria-Martinez A, Susanto E, Peng H, Lehr HA, Delaloye JF, Huelsken J. *Nature*. 2012; 481:85–89.
60. Singh A, Settleman J. *Oncogene*. 2010; 29:4741–4751. [PubMed: 20531305]
61. Sethi T, Rintoul RC, Moore SM, MacKinnon AC, Salter D, Choo C, Chilvers ER, Dransfield I, Donnelly SC, Strieter R, Haslett C. *Nat Med*. 1999; 5:662–668. [PubMed: 10371505]
62. Fornaro M, Plescia J, Chheang S, Tallini G, Zhu YM, King M, Altieri DC, Languino LR. *J Biol Chem*. 2003; 278:50402–50411. [PubMed: 14523021]
63. Pontiggia O, Sampayo R, Raffo D, Motter A, Xu R, Bissell MJ, Joffe EB, Simian M. *Breast Cancer Res Treat*. 2012; 133:459–471. [PubMed: 21935603]
64. Aoudjit F, Vuori K. *Chemotherapy research and practice*. 2012; 2012:283181.
65. Tosoian JJ, Mamawala M, Epstein JI, Landis P, Wolf S, Trock BJ, Carter HB. *Journal of clinical oncology : official journal of the American Society of Clinical Oncology*. 2015; 33:3379–3385. [PubMed: 26324359]
66. Eke I, Storch K, Krause M, Cordes N. *Cancer Res*. 2013; 73:5869–5879. [PubMed: 23950208]
67. Jerhammar F, Ceder R, Garvin S, Grénman R, Grafström RC, Roberg K. *Cancer Biol Ther*. 2014; 10:1244–1251.
68. Ou J, Pan F, Geng P, Wei X, Xie G, Deng J, Pang X, Liang H. *Int J Radiat Oncol Biol Phys*. 2012; 82:e685–691. [PubMed: 22208970]
69. Nam JM, Onodera Y, Bissell MJ, Park CC. *Cancer Res*. 2010; 70:5238–5248. [PubMed: 20516121]
70. Weissleder R, Mahmood U. *Radiology*. 2001; 219:316–333. [PubMed: 11323453]
71. Oon SF, Pennington SR, Fitzpatrick JM, Watson RW. *Nature reviews Urology*. 2011; 8:131–138. [PubMed: 21394176]
72. Hendriks A, Safarik L, Hammerer P. *Eur Urol*. 2002; 41:1–10. [PubMed: 11999460]
73. Santimaria M, Moscatelli G, Viale GL, Giovannoni L, Neri G, Viti F, Leprini A, Borsi L, Castellani P, Zardi L, Neri D, Riva P. *Clin Cancer Res*. 2003; 9:571–579. [PubMed: 12576420]
74. Carnemolla B, Borsi L, Balza E, Castellani P, Meazza R, Berndt A, Ferrini S, Kosmehl H, Neri D, Zardi L. *Blood*. 2002; 99:1659–1665. [PubMed: 11861281]
75. Schliemann C, Palumbo A, Zuberbuhler K, Villa A, Kaspar M, Trachsel E, Klapper W, Menssen HD, Neri D. *Blood*. 2009; 113:2275–2283. [PubMed: 19005180]
76. Wagner K, Schulz P, Scholz A, Wiedenmann B, Menrad A. *Clin Cancer Res*. 2008; 14:4951–4960. [PubMed: 18676770]
77. Weide B, Eigentler TK, Pflugfelder A, Zelba H, Martens A, Pawelec G, Giovannoni L, Ruffini PA, Elia G, Neri D, Gutzmer R, Becker JC, Garbe C. *Cancer immunology research*. 2014; 2:668–678. [PubMed: 24906352]
78. Eigentler TK, Weide B, de Braud F, Spitaleri G, Romanini A, Pflugfelder A, Gonzalez-Iglesias R, Tasciotti A, Giovannoni L, Schwager K, Lovato V, Kaspar M, Trachsel E, Menssen HD, Neri D, Garbe C. *Clin Cancer Res*. 2011; 17:7732–7742. [PubMed: 22028492]
79. Tijink BM, Perk LR, Budde M, Stigter-van Walsum M, Visser GW, Kloet RW, Dinkelborg LM, Leemans CR, Neri D, van Dongen GA. *Eur J Nucl Med Mol I*. 2009; 36:1235–1244.
80. Poli GL, Bianchi C, Virota G, Bettini A, Moretti R, Trachsel E, Elia G, Giovannoni L, Neri D, Bruno A. *Cancer immunology research*. 2013; 1:134–143. [PubMed: 24777501]
81. Halin C, Rondini S, Nilsson F, Berndt A, Kosmehl H, Zardi L, Neri D. *Nat Biotechnol*. 2002; 20:264–269. [PubMed: 11875427]

82. Locher R, Erba PA, Hirsch B, Bombardieri E, Giovannoni L, Neri D, Durkop H, Menssen HD. *Journal of cancer research and clinical oncology*. 2014; 140:35–43. [PubMed: 24132461]
83. Balza E, Mortara L, Sassi F, Monteghirfo S, Carnemolla B, Castellani P, Neri D, Accolla RS, Zardi L, Borsi L. *Clin Cancer Res*. 2006; 12:2575–2582. [PubMed: 16638868]
84. Berndorff D, Borkowski S, Moosmayer D, Viti F, Müller-Tiemann B, Sieger S, Friebe M, Hilger CS, Zardi L, Neri D. *J Nucl Med*. 2006; 47:1707–1716. [PubMed: 17015908]
85. El-Emir E, Dearling JL, Huhlov A, Robson MP, Boxer G, Neri D, van Dongen GA, Trachsel E, Begent RH, Pedley RB. *Br J Cancer*. 2007; 96:1862–1870. [PubMed: 17519905]
86. Rossin R, Berndorff D, Friebe M, Dinkelborg LM, Welch MJ. *J Nucl Med*. 2007; 48:1172–1179. [PubMed: 17574989]
87. Fabbrini M, Trachsel E, Soldani P, Bindi S, Alessi P, Bracci L, Kosmehl H, Zardi L, Neri D, Neri P. *Int J Cancer*. 2006; 118:1805–1813. [PubMed: 16217760]
88. Mariani G, Lasku A, Pau A, Villa G, Motta C, Calcagno G, Taddei GZ, Castellani P, Syrigos K, Dorcaratto A, Epenetos AA, Zardi L, Viale GA. *Cancer*. 1997; 80:2484–2489. [PubMed: 9406699]
89. Mariani G, Lasku A, Balza E, Gaggero B, Motta C, Di Luca L, Dorcaratto A, Viale GA, Neri D, Zardi L. *Cancer*. 1997; 80:2378–2384. [PubMed: 9406686]
90. Frey K, Schliemann C, Schwager K, Giavazzi R, Johannsen M, Neri D. *The Journal of urology*. 2010; 184:2540–2548. [PubMed: 21030045]
91. Moschetta M, Pretto F, Berndt A, Galler K, Richter P, Bassi A, Oliva P, Micotti E, Valbusa G, Schwager K, Kaspar M, Trachsel E, Kosmehl H, Bani MR, Neri D, Giavazzi R. *Cancer Res*. 2012; 72:1814–1824. [PubMed: 22392081]
92. Hemmerle T, Neri D. *Int J Cancer*. 2014; 134:467–477. [PubMed: 23818211]
93. Ye F, Wu X, Jeong EK, Jia Z, Yang T, Parker D, Lu ZR. *Bioconjug Chem*. 2008; 19:2300–2303. [PubMed: 19053180]
94. Gu G, Hu Q, Feng X, Gao X, Menglin J, Kang T, Jiang D, Song Q, Chen H, Chen J. *Biomaterials*. 2014; 35:8215–8226. [PubMed: 24974009]
95. Tan M, Burden-Gulley SM, Li W, Wu X, Lindner D, Brady-Kalnay SM, Gulani V, Lu ZR. *Pharm Res*. 2012; 29:953–960. [PubMed: 22139536]
96. Zhou Z, Qutaish M, Han Z, Schur RM, Liu Y, Wilson DL, Lu ZR. *Nat Commun*. 2015; 6:7984. [PubMed: 26264658]
97. Zhang B, Wang H, Shen S, She X, Shi W, Chen J, Zhang Q, Hu Y, Pang Z, Jiang X. *Biomaterials*. 2016; 79:46–55. [PubMed: 26695116]
98. Simberg D, Duza T, Park JH, Essler M, Pilch J, Zhang L, Derfus AM, Yang M, Hoffman RM, Bhatia S, Sailor MJ, Ruoslahti E. *Proc Natl Acad Sci U S A*. 2007; 104:932–936. [PubMed: 17215365]
99. Peng XH, Qian X, Mao H, Wang AY, Chen ZG, Nie S, Shin DM. *Int J Nanomedicine*. 2008; 3:311–321. [PubMed: 18990940]
100. Zhao J, Zhang B, Shen S, Chen J, Zhang Q, Jiang X, Pang Z. *J Colloid Interface Sci*. 2015; 450:396–403. [PubMed: 25863222]
101. Han Z, Zhou Z, Shi X, Wang J, Wu X, Sun D, Chen Y, Zhu H, Magi-Galluzzi C, Lu ZR. *Bioconjug Chem*. 2015; 26:830–838. [PubMed: 25848940]
102. Han G, Cui Z, Guo B, Mei X. *RSC Advances*. 2016; 6:77321–77328.
103. Sun Y, Kim HS, Park J, Li M, Tian L, Choi Y, Choi BI, Jon S, Moon WK. *Theranostics*. 2014; 4:845–857. [PubMed: 24955145]
104. Saw PE, Kim S, Lee IH, Park J, Yu M, Lee J, Kim JI, Jon S. *Journal Of Materials Chemistry B*. 2013; 1:4723–4726.
105. Kim H, Lee Y, Lee IH, Kim S, Kim D, Saw PE, Lee J, Choi M, Kim YC, Jon S. *J Control Release*. 2014; 178:118–124. [PubMed: 24462899]
106. Sun Y, Kim HS, Saw PE, Jon S, Moon WK. *Adv Healthc Mater*. 2015; 4:1675–1680. [PubMed: 26097122]
107. Carnemolla B, Balza E, Siri A, Zardi L, Nicotra MR, Bigotti A, Natali PG. *J Cell Biol*. 1989; 108:1139–1148. [PubMed: 2646306]

108. Balza E, Sassi F, Ventura E, Parodi A, Fossati S, Blalock W, Carnemolla B, Castellani P, Zardi L, Borsi L. *Int J Cancer*. 2009; 125:751–758. [PubMed: 19479996]
109. Ventura E, Sassi F, Parodi A, Balza E, Borsi L, Castellani P, Carnemolla B, Zardi L. *Plos One*. 2010; 5:e9145. [PubMed: 20161770]
110. Pini A, Viti F, Santucci A, Carnemolla B, Zardi L, Neri P, Neri D. *J Biol Chem*. 1998; 273:21769–21776. [PubMed: 9705314]
111. Borsi L, Balza E, Bestagno M, Castellani P, Carnemolla B, Biro A, Leprini A, Sepulveda J, Burrone O, Neri D, Zardi L. *Int J Cancer*. 2002; 102:75–85. [PubMed: 12353237]
112. Villa A, Trachsel E, Kaspar M, Schliemann C, Somavilla R, Rybak JN, Rosli C, Borsi L, Neri D. *Int J Cancer*. 2008; 122:2405–2413. [PubMed: 18271006]
113. Zahnd C, Kawe M, Stumpp MT, de Pasquale C, Tamaskovic R, Nagy-Davidescu G, Dreier B, Schibli R, Binz HK, Waibel R, Pluckthun A. *Cancer Res*. 2010; 70:1595–1605. [PubMed: 20124480]
114. Kim S, Kim D, Jung HH, Lee IH, Kim JI, Suh JY, Jon S. *Angewandte Chemie*. 2012; 51:1890–1894. [PubMed: 22271427]
115. Pilch J, Brown DM, Komatsu M, Jarvinen TA, Yang M, Peters D, Hoffman RM, Ruoslahti E. *Proc Natl Acad Sci U S A*. 2006; 103:2800–2804. [PubMed: 16476999]
116. Sutcliffe-Goulden JL, O'Doherty MJ, Marsden PK, Hart IR, Marshall JF, Bansal SS. *Eur J Nucl Med Mol Imaging*. 2002; 29:754–759. [PubMed: 12029548]
117. D'Souza CA, McBride WJ, Sharkey RM, Todaro LJ, Goldenberg DM. *Bioconjug Chem*. 2011; 22:1793–1803. [PubMed: 21805975]
118. Tan MQ, Ye Z, Jeong EK, Wu XM, Parker DL, Lu ZR. *Bioconjug Chem*. 2011; 22:931–937. [PubMed: 21473650]
119. Zhou Z, Wu X, Kresak A, Griswold M, Lu ZR. *Biomaterials*. 2013; 34:7683–7693. [PubMed: 23863450]
120. Ye F, Jeong EK, Parker D, Lu ZR. *Bo pu xue za zhi= Chinese journal of microwave & radio-frequency spectroscopy/Zhongguo wu li xue hui bo pu xue zhuan ye wei yuan hui bian ji*. 2011; 2:325.
121. Wu X, Lindner D, Yu GP, Brady-Kalnay S, Lu ZR. *Journal of visualized experiments : JoVE*. 2013
122. Wu X, Burden-Gulley SM, Yu GP, Tan M, Lindner D, Brady-Kalnay SM, Lu ZR. *Bioconjug Chem*. 2012; 23:1548–1556. [PubMed: 22812444]
123. Wu X, Yu G, Lindner D, Brady-Kalnay SM, Zhang Q, Lu ZR. *Am J Nucl Med Mol Imaging*. 2014; 4:525–536. [PubMed: 25250202]
124. Park J, Kim S, Saw PE, Lee IH, Yu MK, Kim M, Lee K, Kim YC, Jeong YY, Jon S. *J Control Release*. 2012; 163:111–118. [PubMed: 22964395]
125. Neri D, Carnemolla B, Nissim A, Leprini A, Querzè G, Balza E, Pini A, Tarli L, Halin C, Neri P. *Nat Biotechnol*. 1997; 15:1271–1275. [PubMed: 9359110]
126. Graf K, Dietrich T, Tachezy M, Scholle FD, Licha K, Stawowy P, Grafe M, Hauff P, Fleck E. *Mol Imaging*. 2008; 7:68–76. [PubMed: 18706289]
127. Vollmer S, Vater A, Licha K, Gemeinhardt I, Gemeinhardt O, Voigt J, Ebert B, Schnorr J, Taupitz M, Macdonald R, Schirner M. *Mol Imaging*. 2009; 8:330–340. [PubMed: 20003891]
128. Matter CM, Schuler PK, Alessi P, Meier P, Ricci R, Zhang D, Halin C, Castellani P, Zardi L, Hofer CK, Montani M, Neri D, Luscher TF. *Circ Res*. 2004; 95:1225–1233. [PubMed: 15539632]
129. Tijink BM, Neri D, Leemans CR, Budde M, Dinkelborg LM, Stigter-van Walsum M, Zardi L, van Dongen GA. *J Nucl Med*. 2006; 47:1127–1135. [PubMed: 16818947]
130. Sauer S, Erba PA, Petrini M, Menrad A, Giovannoni L, Grana C, Hirsch B, Zardi L, Paganelli G, Mariani G. *Blood*. 2009; 113:2265–2274. [PubMed: 19131554]
131. Moosmayer D, Berndorff D, Chang CH, Sharkey RM, Rother A, Borkowski S, Rossi EA, McBride WJ, Cardillo TM, Goldenberg DM, Dinkelborg LM. *Clin Cancer Res*. 2006; 12:5587–5595. [PubMed: 17000696]

132. Zhang B, Shen S, Liao Z, Shi W, Wang Y, Zhao J, Hu Y, Yang J, Chen J, Mei H, Hu Y, Pang Z, Jiang X. *Biomaterials*. 2014; 35:4088–4098. [PubMed: 24513320]
133. Lo KM, Lan Y, Lauder S, Zhang J, Brunkhorst B, Qin G, Verma R, Courtenay-Luck N, Gillies SD. *Cancer immunology, immunotherapy : CII*. 2007; 56:447–457. [PubMed: 16874486]
134. Rudman SM, Jameson MB, McKeage MJ, Savage P, Jodrell DI, Harries M, Acton G, Erlandsson F, Spicer JF. *Clin Cancer Res*. 2011; 17:1998–2005. [PubMed: 21447719]
135. Borsi L, Balza E, Carnemolla B, Sassi F, Castellani P, Berndt A, Kosmehl H, Biro A, Siri A, Orecchia P, Grassi J, Neri D, Zardi L. *Blood*. 2003; 102:4384–4392. [PubMed: 12933583]
136. Halin C, Gafner V, Villani ME, Borsi L, Berndt A, Kosmehl H, Zardi L, Neri D. *Cancer Res*. 2003; 63:3202–3210. [PubMed: 12810649]
137. Pretto F, Elia G, Castioni N, Neri D. *Cancer immunology, immunotherapy : CII*. 2014; 63:901–910. [PubMed: 24893857]
138. Hemmerle T, Probst P, Giovannoni L, Green AJ, Meyer T, Neri D. *Br J Cancer*. 2013; 109:1206–1213. [PubMed: 23887603]
139. Spitaleri G, Berardi R, Pierantoni C, De Pas T, Noberasco C, Libbra C, Gonzalez-Iglesias R, Giovannoni L, Tasciotti A, Neri D, Menssen HD, de Braud F. *Journal of cancer research and clinical oncology*. 2013; 139:447–455. [PubMed: 23160853]
140. Papadia F, Basso V, Patuzzo R, Maurichi A, Di Florio A, Zardi L, Ventura E, Gonzalez-Iglesias R, Lovato V, Giovannoni L, Tasciotti A, Neri D, Santinami M, Menssen HD, De Cian F. *J Surg Oncol*. 2013; 107:173–179. [PubMed: 22674435]
141. Danielli R, Patuzzo R, Di Giacomo AM, Gallino G, Maurichi A, Di Florio A, Cutaia O, Lazzeri A, Fazio C, Miracco C, Giovannoni L, Elia G, Neri D, Maio M, Santinami M. *Cancer immunology, immunotherapy : CII*. 2015; 64:999–1009. [PubMed: 25971540]
142. Freire-de-Lima L, Gelfenbeyn K, Ding Y, Mandel U, Clausen H, Handa K, Hakomori SI. *Proc Natl Acad Sci U S A*. 2011; 108:17690–17695. [PubMed: 22006308]
143. Gujrati M, Vaidya A, Lu ZR. *Bioconjug Chem*. 2016; 27:19–35. [PubMed: 26629982]
144. Bobbin ML, Rossi JJ. *Annual review of pharmacology and toxicology*. 2016; 56:103–122.
145. Wentink MQ, Huijbers EJ, de Gruijl TD, Verheul HM, Olsson AK, Griffioen AW. *Biochim Biophys Acta*. 2015; 1855:155–171. [PubMed: 25641676]
146. Huijbers EJ, Ringvall M, Femel J, Kalamajski S, Lukinius A, Abrink M, Hellman L, Olsson AK. *FASEB journal : official publication of the Federation of American Societies for Experimental Biology*. 2010; 24:4535–4544. [PubMed: 20634349]
147. Femel J, Huijbers EJ, Saupe F, Cedervall J, Zhang L, Roswall P, Larsson E, Olofsson H, Pietras K, Dimberg A, Hellman L, Olsson AK. *Oncotarget*. 2014; 5:12418–12427. [PubMed: 25360764]
148. Ahn S, Lee IH, Kang S, Kim D, Choi M, Saw PE, Shin EC, Jon S. *Advanced Healthcare Materials*. 2014; 3:1194–1199. [PubMed: 24652754]
149. Lucky SS, Soo KC, Zhang Y. *Chem Rev*. 2015; 115:1990–2042. [PubMed: 25602130]

Biographies



Zheng Han obtained his bachelor's degree from the Department of Chemical Engineering, Tianjin University. He is now a PhD candidate in Prof. Zheng-Rong Lu's group in the

Department of Biomedical Engineering, Case Western Reserve University. His research interests include biomaterials, molecular imaging and drug delivery.



Dr. Zheng-Rong Lu is M. Frank Rudy and Margaret Domiter Rudy Professor of Biomedical Engineering at the Department of Biomedical Engineering, Case Western Reserve University. Dr. Lu received his B.S. and M.S. in Chemistry from Lanzhou University, and Ph.D. in Chemistry from Lanzhou Institute of Chemical Physics, Chinese Academy of Sciences at Lanzhou, China. In 1992, Dr. Lu was recruited as Associate Professor of Chemistry and promoted to Professor of Chemistry shortly after at Wuhan University in China. In 2002, Dr. Lu was recruited as Assistant Professor in the Department of Pharmaceutics and Pharmaceutical Chemistry at the University of Utah, and was promoted to a tenured Associate Professor in 2006. He has been in CWRU since 2009. Dr. Lu's research efforts involve molecular imaging, novel MRI contrast agents, and pH-sensitive multifunctional lipids for delivery of nucleic acids.

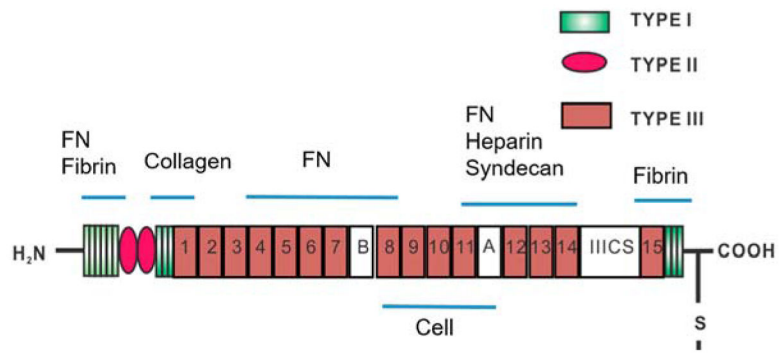


Figure 1. Fibronectin structure and its binding sites to cell and other ECM molecules. Extradomains in insoluble FNs (EDA, EDB and IIICS) are denoted by white blocks between other type III domains.

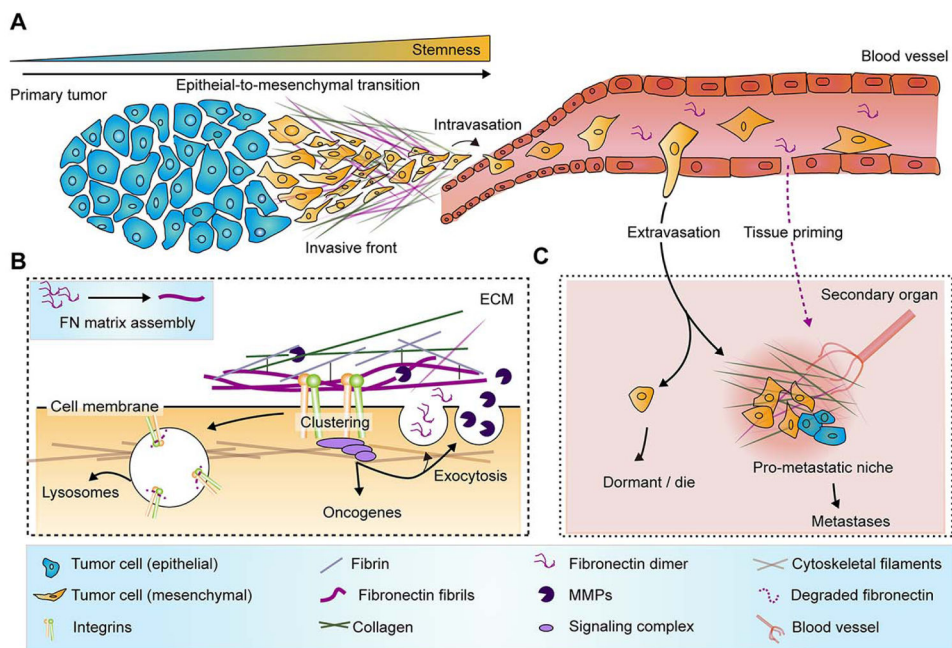


Figure 2.

Upregulation of FN is crucial for cancer survival, invasion, and metastasis. **A.** FN is upregulated in the invasive front of primary tumor, which mainly comprises of cancer cells of mesenchymal phenotype. Epithelial-to-mesenchymal transition (EMT) is responsible for generating cells of increased stemness. These stem-like cells, which are enriched in the invasive front, are prone to disseminate to secondary organs. Abundantly expressed FN and other ECM molecules in the invasive front form a unique tumor microenvironment that promotes the migration and extravasation of cancer cells. **B.** FN serves as a central organizer of ECM molecules and mediates the crosstalk between tumor microenvironment and cancer cells. In malignant cancer cells, FN assembles into FN matrix mediated by the clustering of integrins. FN matrix provides docking sites for collagen and fibrin, and assists the formation and organization of the extracellular matrix. Clustering of integrin, facilitated by FN matrix, also activates intracellular signaling complexes that activate a cascade of oncogenes. This also promotes the expression and secretion of more FNs, MMPs, and other tumor-promoting factors, such as TGF β . MMPs modulate the regulated degradation of FN, collagen, and fibrin matrix, and the degraded products are endocytosed with the aid of integrins. **C.** A receptive microenvironmental feature of upregulated FN in the secondary organ is essential for the metastases formation. Extravasated cancer cells in the secondary organ are faced with two fates: (1) dormancy and death if they are arrested in tissues lack of a favorable microenvironment, or (2) proliferation and metastases if they are engrafted in pro-metastatic niche enriched with FN, collagen, fibrin, etc. Subsequently, the cells may go through mesenchymal-to-epithelial transition (MET) for outgrowth. FN originated from primary tumor may be used to prime tissue where pro-metastatic niche is formed.

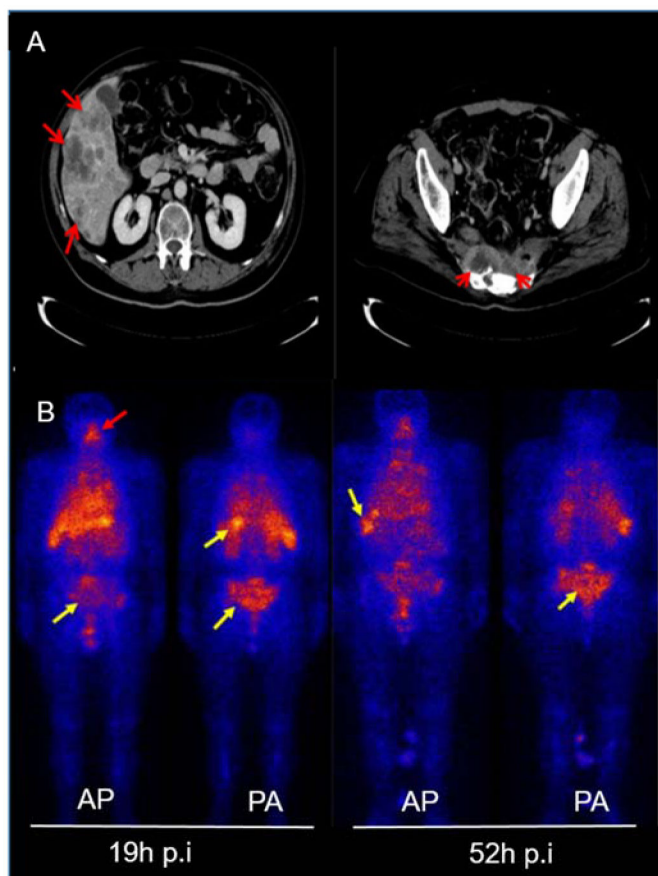


Figure 3. Tumor uptake of ^{131}I -L19SIP in a patient with metastatic prostate cancer. **A.** CT scans confirmed the presence of G3 prostate cancer in the sacrum, the lower spine, and his right lobe of liver as indicated with arrows. **B.** A diagnostic dose of ^{131}I -L19SIP was administered intravenously and whole-body planar images (anterior, left; posterior, right) were taken at post injection. Uptake of ^{131}I -L19SIP is indicated in orange color, which is present in the oscastrum, lower spine, liver and mediastinum 19 and 52 h post injection (p.i). Nonspecific uptake to the oropharygea mucosal linings is indicated with red arrow. Images of anterior posterior (AP) position and posterior anterior (PA) position were shown. Adapted and reprinted with permission based on ref. 80.

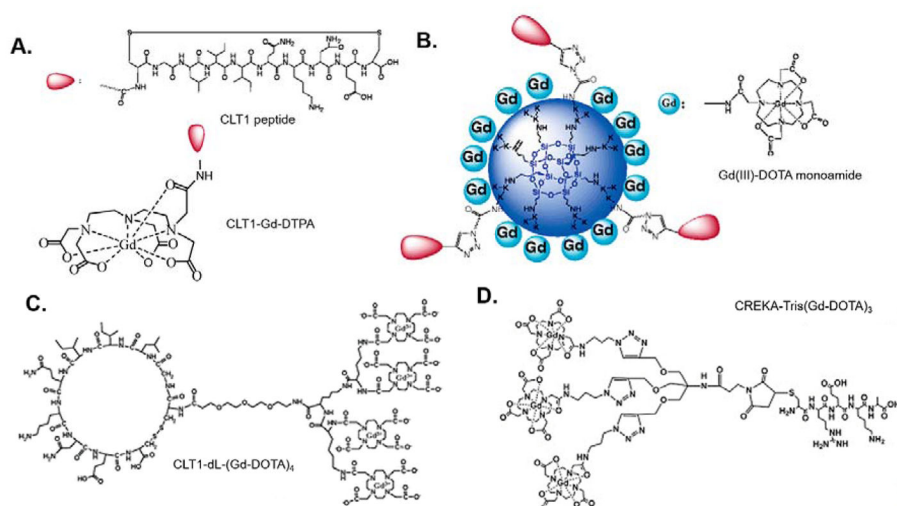


Figure 4.

MRI contrast agents based on FN-targeting peptides. **A.** Chemical structures of CLT1-Gd-DTPA. The compound was synthesized in solid phase by directly conjugating Gd-DTPA to the N-terminal of the cyclic CLT1 peptide, with the sequence of CGLIQKNEC. **B.** Structure of CLT1-G2-(Gd-DOTA). The structure encircled by the dark blue sphere denotes Generation 2 (G2) nanoglobule polylysine dendrimer, which was modified with Gd-DOTA. CLT1 peptide was conjugated to the nanoglobule through click chemistry. **C.** Chemical structure CLT1-dL-(Gd-DOTA)₄, which contains four Gd-DOTA monoamide chelates and CLT1 targeting peptide. **D.** Chemical structure of CREKA-Tris(Gd-DOTA)₃. The compound was synthesized by conjugating CREKA and azide bearing Gd-DOTA to the maleimide-functionalized trialkyne scaffold through thiol-maleimide and azid-alkyne click chemistry, respectively. The aforementioned structures were adapted with permission based on ref. ^{93, 95, 122 and 119}, respectively.

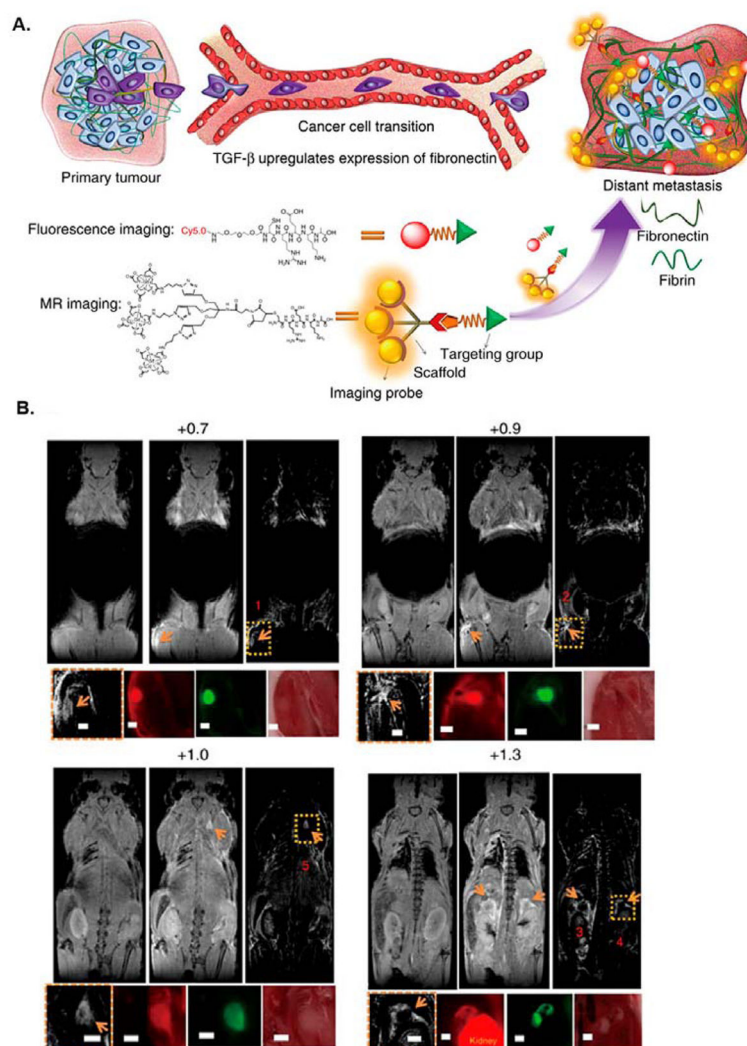


Figure 5. MRI detection of breast cancer micrometastases using FibFN targeting contrast agent, CREKA-Tris(Gd-DOTA)₃. **A.** Breast cancer metastasis is accompanied by upregulated FN expression in metastases. By targeting overexpressed FN, which forms complexes with fibrin, CREKA-Tris(Gd-DOTA) accumulates at a high concentration in sites of metastases, resulting significant tumor enhancement in MRI, which is validated by high-resolution fluorescence imaging of CREKA-Cy5 also accumulated in metastases. **B.** MRI images of breast cancer micrometastases contrast enhanced with CREKA-Tris(Gd-DOTA)₃ show the coronal slices before and after CREKA-Tris(Gd-DOTA)₃ injection, the subtraction images of the pre-injection from the post-injection images, and the enlarged subtraction MRI images of metastatic sites. Corresponding GFP cryo-fluorescence images of the micrometastases and CREKA-Cy5.0 images validate the MRI detection of micrometastases (tumors are indicated by arrow; all scale bars, 1mm). Adapted and reprinted with permission based on ref. ⁹⁶.

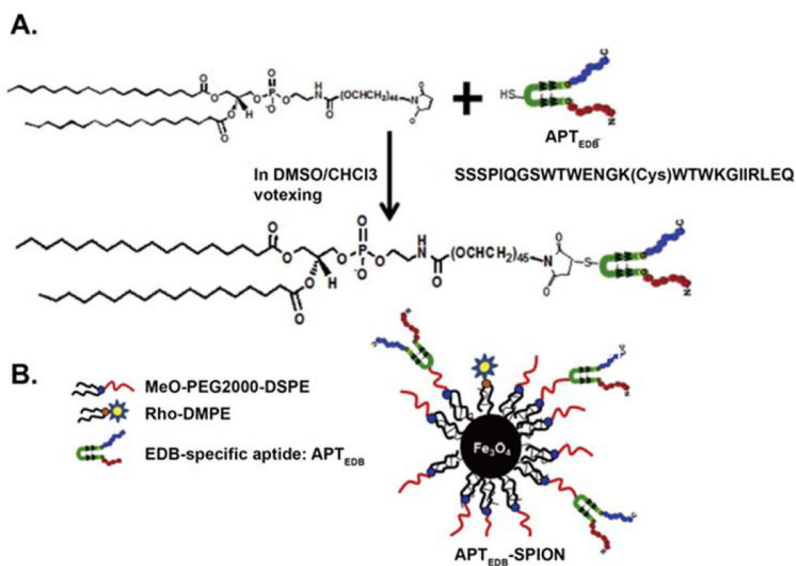


Figure 6. EDB-FN specific peptide, APT_{EDB}, modified superparamagnetic iron oxide nanoparticles as targeted MRI contrast agents. **A.** Functionalizing APT_{EDB} for labeling nanoparticles. **B.** A schematic depiction of APT_{EDB}-SPION nanoparticle for T₂*-weighted MRI. Adapted and reprinted with permission based on ref. ^{103, 124}.

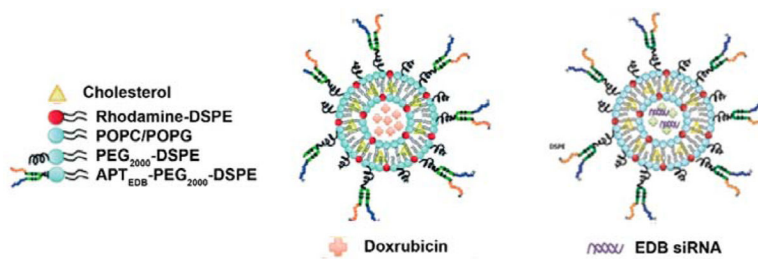


Figure 7. Structural illustration of APT_{EDB}-modified liposomes for delivery of doxorubicin and anti-EDB siRNA. Adapted and reprinted with permission based on ref. 117 and 138.

Table 1

FN-targeting ligands and their application in cancer imaging and therapy

Ligand	Form	Target	Cargo	Imaging agents		Therapeutics	
				Modality	Application	Cargo	Application
L19	mAb	EDB	¹²⁵ I	Nuclear	Brain ⁷³ , lung ⁷³ , and colon ⁷³ cancers	IL-2	Teratocarcinoma ⁷⁴ , lymphoma ⁷⁵ , pancreatic cancer ⁷⁶ , melanoma ^{77, 78}
			¹²⁴ I	Nuclear	Head and neck cancer ⁷⁹ , brain metastases ⁸⁰	IL-12	Lung cancer ⁸¹
			¹³¹ I	Nuclear	Prostate cancer ⁸²	TNF	Teratocarcinoma ¹²⁸ , fibrosarcoma ⁸³ , colon cancer, sarcoma ¹³⁰ and melanoma ¹³¹
			^{99m} Tc	Nuclear	Teratocarcinoma ⁸⁴	¹³¹ I	Brain ⁸⁰ , colon ⁸⁵ , and prostate cancer ⁸²
			⁷⁶ Br	Nuclear	Teratocarcinoma ⁸⁶	SnChe ₆	Fibroblast sarcoma ⁸⁷ , teratocarcinoma ⁸⁷ , colon cancer ⁸⁷
BC-1	mAb	⁷ FNIII	^{99m} Tc	Nuclear	Glioma ⁸⁸	¹²⁵ I	Human tumor implants ⁸⁹
F8	mAb	EDA				IL-12	Skin ¹⁰⁴ , renal ¹⁰⁴ , and prostate cancers ¹⁰⁴
						IL2	Renal ⁹⁰ , skin ⁹¹ , and colon cancers ⁹² , lymphoma ⁹² , teratocarcinoma ⁹²
CLT1	peptide	FibFN	Gd-DTPA	MRI	Colon cancer ⁹³ , breast cancer ⁹⁴	IL12	Glioma ⁹⁴
			G2-(Gd-DOTA) ₄	MRI	Prostate cancer ⁹⁵	PTX loaded NP	
			(Gd-DOTA) ₄	MRI	Prostate cancer ^{95,96,97}		
CLT2	peptide	FibFN					
CREKA	peptide	FibFN	Tris(Gd-DOTA) ₄	MRI	Breast cancer ^{93,96}	MWNTs-PEG	Lung cancer ⁹⁷
			SPION	MRI	Breast cancer ^{98,99}	PAMAM	Glioma ¹⁰⁰
ZD2	peptide	EDB			Prostate cancer ¹⁰¹	DOX	Prostate cancer ¹⁰²
APT _{EDB}	peptide	EDB	SPION	MRI	Breast cancer ¹⁰³	DOX loaded NP	Glioma ¹⁰⁴
						PTX loaded NP	Glioma ⁹⁴
						DTX	Glioma ¹⁰⁵
						siEDB loaded NP	Breast cancer ¹⁰⁶